

# SCIENTIFIC REPORTS



OPEN

## *In-situ* observation of ultrafast 90° domain switching under application of an electric field in (100)/(001)-oriented tetragonal epitaxial $\text{Pb}(\text{Zr}_{0.4}\text{Ti}_{0.6})\text{O}_3$ thin films

Received: 7 March 2017

Accepted: 26 July 2017

Published online: 29 August 2017

Yoshitaka Ehara<sup>1</sup>, Shintaro Yasui<sup>2</sup>, Takahiro Oikawa<sup>1</sup>, Takahisa Shiraishi<sup>1,3</sup>, Takao Shimizu<sup>4,5</sup>, Hiroki Tanaka<sup>1</sup>, Noriyuki Kanenko<sup>1</sup>, Ronald Maran<sup>6</sup>, Tomoaki Yamada<sup>7,8</sup>, Yasuhiko Imai<sup>9</sup>, Osami Sakata<sup>1,10</sup>, Nagarajan Valanoor<sup>6</sup> & Hiroshi Funakubo<sup>1,4,5</sup>

Ferroelastic domain switching significantly affects piezoelectric properties in ferroelectric materials. The ferroelastic domain switching and the lattice deformation of both  $a$ -domains and  $c$ -domains under an applied electric field were investigated using *in-situ* synchrotron X-ray diffraction in conjunction with a high-speed pulse generator set up for epitaxial (100)/(001)-oriented tetragonal  $\text{Pb}(\text{Zr}_{0.4}\text{Ti}_{0.6})\text{O}_3$  (PZT) films grown on  $(100)\text{SrRuO}_3//(100)\text{KTaO}_3$  substrates. The  $004$  peak ( $c$ -domain) position shifts to a lower  $2\theta$  angle, which demonstrates the elongation of the  $c$ -axis lattice parameter of the  $c$ -domain under an applied electric field. In contrast, the  $400$  peak ( $a$ -domain) shifts in the opposite direction (higher angle), thus indicating a decrease in the  $a$ -axis lattice parameter of the  $a$ -domain. 90° domain switching from (100) to (001) orientations (from  $a$ -domain to  $c$ -domain) was observed by a change in the intensities of the  $400$  and  $004$  diffraction peaks by applying a high-speed pulsed electric field 200 ns in width. This change also accompanied a tilt in the angles of each domain from the substrate surface normal direction. This behaviour proved that the 90° domain switched within 40 ns under a high-speed pulsed electric field. Direct observation of such high-speed switching opens the way to design piezo-MEMS devices for high-frequency operation.

Ferroelectric materials have been applied to many electronic devices, including sensors and actuators. Because of their superior piezoelectric and ferroelectric properties,  $\text{Pb}(\text{Zr}_{1-x}\text{Ti}_x)\text{O}_3$  thin films have been extensively studied for microelectromechanical system [MEMS] applications<sup>1</sup>. It has been pointed out that the electromechanical response of  $\text{Pb}(\text{Zr}_{1-x}\text{Ti}_x)\text{O}_3$  is composed of not only lattice elongation (so-called intrinsic contribution of piezoresponse) but also extrinsic contributions, which include the motion of the domain walls, separating ferroelastic domains (non-180° domain motion) under an applied electric field, for example, switching from (100)- to (001)-orientated domains (90° domain switching) in tetragonal  $\text{Pb}(\text{Zr}_{1-x}\text{Ti}_x)\text{O}_3$  films<sup>2</sup>. In particular, the extrinsic contributions are responsible for more than 50% of the total piezoelectric response, as well as the dielectric response<sup>3</sup>. Therefore, non-180° ferroelastic domain switching induced by the application of an electric field is a

<sup>1</sup>Department of Innovative and Engineered Material, Tokyo Institute of Technology, Yokohama, 226-8502, Japan.

<sup>2</sup>Laboratory for Materials and Structures, Tokyo Institute of Technology, Yokohama, 226-8503, Japan. <sup>3</sup>Institute for Materials Research, Tohoku University, 2-1-1 Katahira, Aoba-ku, Sendai, 980-8577, Japan.

<sup>4</sup>Materials Research Center for Element Strategy, Tokyo Institute of Technology, Yokohama, 226-8503, Japan. <sup>5</sup>School of Materials and Chemical Technology, Tokyo Institute of Technology, Yokohama, 226-8502, Japan. <sup>6</sup>School of Materials Science and Engineering, University of New South Wales, NSW 2052, Sydney, Australia. <sup>7</sup>Department of Materials, Physics and Energy Engineering, Nagoya University, Nagoya, 464-8603, Japan. <sup>8</sup>PRESTO, Japan Science and Technology Agency, 4-1-8 Honcho, Kawaguchi, Saitama, 332-0012, Japan. <sup>9</sup>Japan Synchrotron Radiation Research Institute (JASRI), 1-1-1 Kouto, Sayo-cho, Sayo-gun, Hyogo, 679-5198, Japan. <sup>10</sup>Synchrotron X-ray Station at SPring-8 and Synchrotron X-ray Group, National Institute for Materials Science (NIMS), 1-1-1 Kouto, Sayo, Hyogo, 679-5148, Japan. Correspondence and requests for materials should be addressed to H.F. (email: [funakubo.haa@m.titech.ac.jp](mailto:funakubo.haa@m.titech.ac.jp))

significant feature and is required for the design of high-performance piezoelectric devices for MEMS applications. Much efforts have been devoted to clarify the dynamics of the non-180° ferroelastic domain in epitaxial  $\text{Pb}(\text{Zr}_{1-x}\text{Ti}_x)\text{O}_3$  films<sup>4–9</sup>. The change in the non-180° ferroelastic domain structure with the application of an electric field has been investigated using various techniques, such as transmission electron microscopy (TEM)<sup>6,9</sup>, piezoresponse force microscopy (PFM)<sup>4,7,8</sup>, and X-ray diffraction (XRD)<sup>5</sup> for polydomain (100)/(001)-oriented epitaxial tetragonal  $\text{Pb}(\text{Zr}_{1-x}\text{Ti}_x)\text{O}_3$  films. The domain structures strongly depend on the film thickness and substrate<sup>10–12</sup>, and the  $\text{Zr}/(\text{Zr} + \text{Ti})$  ratio in the films<sup>13</sup>, as well as the poling treatment.

The dynamics of the crystal lattice while applying an electric field in  $\text{Pb}(\text{Zr}_{1-x}\text{Ti}_x)\text{O}_3$  films have been measured by *in-situ* XRD measurement<sup>14–17</sup>. Lattice elongation and 180° domain wall motion were observed at sub-nanosecond timescales for (001)-oriented  $\text{Pb}(\text{Zr}_{1-x}\text{Ti}_x)\text{O}_3$  thin films<sup>14,15</sup>, and it has been reported that non-180° ferroelastic domains can be switched by application of an electric field on the order of hundreds of nanoseconds<sup>16,17</sup> in ferroelectric films. However, it has not been clarified yet how fast does the 90° domain switching proceed - in particular, the relationship between the lattice elongation and geometrical domain structure deformation in tetragonal  $\text{Pb}(\text{Zr}_{1-x}\text{Ti}_x)\text{O}_3$  thin films has not been determined from a response speed point of view.

In the present study, we investigated the change in lattice parameters and domain structure for 600-nm thick (100)/(001)-oriented epitaxial tetragonal  $\text{Pb}(\text{Zr}_{0.4}\text{Ti}_{0.6})\text{O}_3$  films, which were subjected to an applied rectangular electric field pulses of 200-ns and rest time of 800 ns. The average lattice parameters and domain structure of the films under this electric field was then determined using a time-resolved *in-situ* synchrotron X-ray diffraction system in conjunction with a high-speed pulse generator. We show that in contrast to conventionally accepted scenario of sluggish nature of ferroelastic domain switching as pointed out in ceramics<sup>18</sup>, simultaneous lattice deformation ( $c$ -axis and  $a$ -axis) and ferroelastic domain switching ( $c$ -domain volume fraction and geometrical twin 90° domain structure) occurs on the order of sub-microseconds.

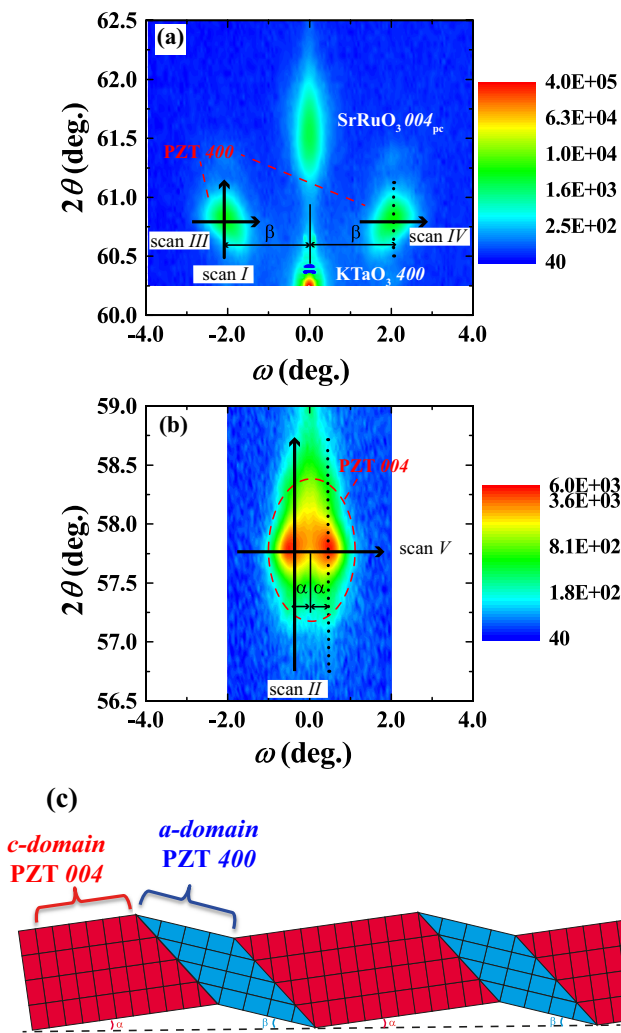
## Results and Discussion

High-resolution X-ray diffraction (HRXRD)  $2\theta-\omega$  mappings around the PZT 400 and 004 diffraction peaks of (100)/(001)-oriented epitaxial PZT films grown on (100) $_{\text{SrRuO}_3}$ //(100) $_{\text{KTaO}_3}$  substrates are shown in Fig. 1(a) and (b), respectively. Split PZT 400 diffractions as twin peaks ( $a$ -domains) are observed in Fig. 1(a), together with  $\text{SrRuO}_3$  400<sub>c</sub> and  $\text{KTaO}_3$  400 diffraction peaks, while split PZT 004 diffractions as twin peaks ( $c$ -domains) are observed in Fig. 1(b). This tilted domain structure has been examined in a number of reports using cross-sectional TEM or X-ray rocking curve analysis<sup>10–13,19–24</sup>. The twin peaks split in the rocking curve direction ( $\omega$ -axis), the horizontal axis in Fig. 1(a) and (b), are observed because of the tetragonality of the film structure<sup>10,12</sup>. The tilting angles of  $c$ -domains ( $\beta$  angle) and  $a$ -domains ( $\alpha$  angle) can be interpreted by considering that the films are required to be attached to a flat surface substrate, as illustrated in Fig. 1(c). Angles of  $\alpha = 0.41^\circ$  and  $\beta = 1.96^\circ$  were obtained from the  $2\theta-\omega$  mappings shown in Fig. 1(a) and (b), respectively. It must be mentioned that the disoriented angles from the substrate surface have been ascertained to depend on the volume fraction of the  $c$ -domain ( $V_c$ )<sup>22</sup> and the tetragonality ( $c/a$  ratio), as described in supplementary materials<sup>12</sup>.

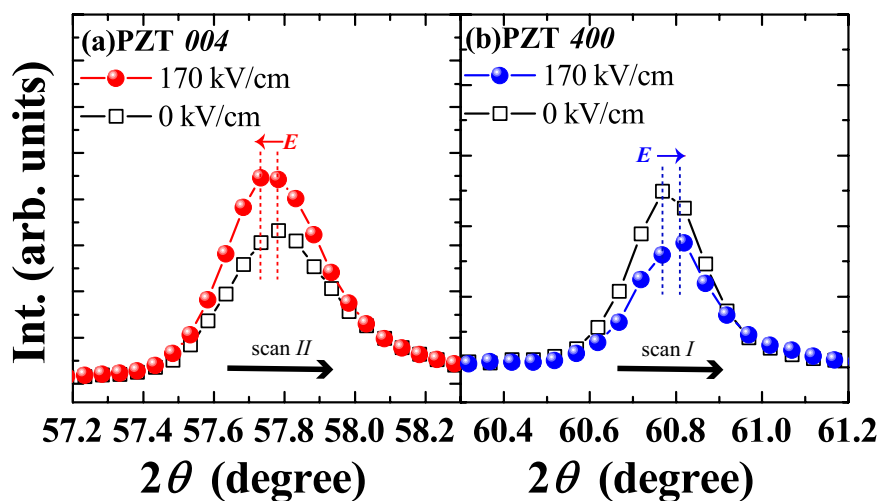
Figure 2(a) and (b) show HRXRD  $2\theta-\omega$  scans for PZT 004 [scan II in Fig. 1(b)] and PZT 400 [scan I in Fig. 1(a)] measured by the application of a 200-ns pulsed electric field with an amplitude of 170 kV/cm and zero field. The PZT 004 peak shifted to a lower  $2\theta$  angle, which demonstrates the elongation of the surface normal  $c$ -axis lattice parameter of the  $c$ -domain, with an applied electric field. On the other hand, the PZT 400 peaks shifted in the opposite direction (higher  $2\theta$  angle), as shown in Fig. 2(b), indicating a decrease in the surface normal  $a$ -axis lattice parameter of the  $a$ -domain under an applied electric field. This elongation of the surface normal  $c$ -axis lattice parameter of the  $c$ -domain and decrease in the surface normal  $a$ -axis lattice parameter of the  $a$ -domain occurs simultaneously. Moreover, a clear difference in the intensities of both PZT 004 and PZT 400 diffraction peaks between 0 V (before applying an electric field) and 170 kV/cm (under applying an electric field) is found. This result is direct evidence of 90° domain switching from (100) to (001) orientation, as is the increase in  $V_c$  during a 200-ns-wide pulsed electric field. The application of an electric field forces ferroelectric/ferroelastic domains to move towards the direction parallel to the electric field to minimise the total energy in the film. It must be noted that the decrease in the lattice spacing along the  $a$ -axis of  $a$ -domain that is perpendicular to the polarization direction can be understood by the shear deformation owing to none-zero piezoelectric tensor  $d_{15}$ <sup>25</sup>. The appreciable  $d_{15}$  response in the  $a$ -domain may be also associated with the change of domain fraction by the electric field. Full understanding of the geometrical correlation between  $a$ - and  $c$ -domains under the electric field will be reported in the future.

Figure 3 shows the change in the rocking curve scans ( $\omega$  scans) for the  $c$ -domain [scan V in Fig. 1(b)] and  $a$ -domain [scans III and IV in Fig. 1(a)] under an applied 200-ns-wide pulsed electric field. The tilting angle of the PZT 004 twin peaks decreased, as shown in the Fig. 3(a). This motion indicates decreasing  $\alpha$  angles of the  $c$ -domains ( $\Delta\alpha$ ), which is accompanied by an increase in  $V_c$  under the applied electric field, in agreement with Fig. 2. On the other hand, as shown in Fig. 3(b) and (c), the PZT 400 peaks were shifted to lower and higher angles, respectively, which indicate an increase in the  $\beta$  angle of the  $a$ -domains ( $\Delta\beta$ ) under the application of an electric field. Thus the time-resolved *in-situ* XRD measurements show direct evidence of a dynamic increase of the  $V_c$  and lattice parameters as well as changing tilting angle of each domain with the application of an electric field.

We now discuss the time response of the changes in the lattice parameters,  $V_c$ , and the tilting angle of the domains with respect to an electric field. Figure 4 shows the electric charge (Fig. 4(a)), the lattice strains (Fig. 4(b)), the tilting angles (Fig. 4(c)), and the peak intensity of each domain (Fig. 4(d)) as a function of time. The electrical charges were plotted every 2 ns, while others were every 20 ns to obtain sufficient intensity for analysis. These data were obtained by fitting with Gaussian functions except for Fig. 4(a). An imperfect rectangular shape of the charge with respect to an applied electric pulse is shown in Fig. 4(a) when a 200-ns-wide pulsed voltage with amplitude of 170 kV/cm was applied to the PZT films. To further visualise this in detail, the time



**Figure 1.** HRXRD  $2\theta$ - $\omega$  mappings near (a) PZT 400 and (b) PZT 004 for (100)/(001)-oriented epitaxial tetragonal  $\text{Pb}(\text{Zr}_{0.4}\text{Ti}_{0.6})\text{O}_3$  films. (c) Schematic representation of the domain structure.



**Figure 2.** HRXRD  $2\theta$  scans of (a) PZT 004 [scan II in Fig. 1(b)] and (b) PZT 400 [scan I in Fig. 1(a)] measured under a 200-ns pulsed electric field with amplitudes of 0 kV/cm (open squares) and 170 kV/cm (filled circles) for the same  $\text{Pb}(\text{Zr}_{0.4}\text{Ti}_{0.6})\text{O}_3$  films shown in Fig. 1.

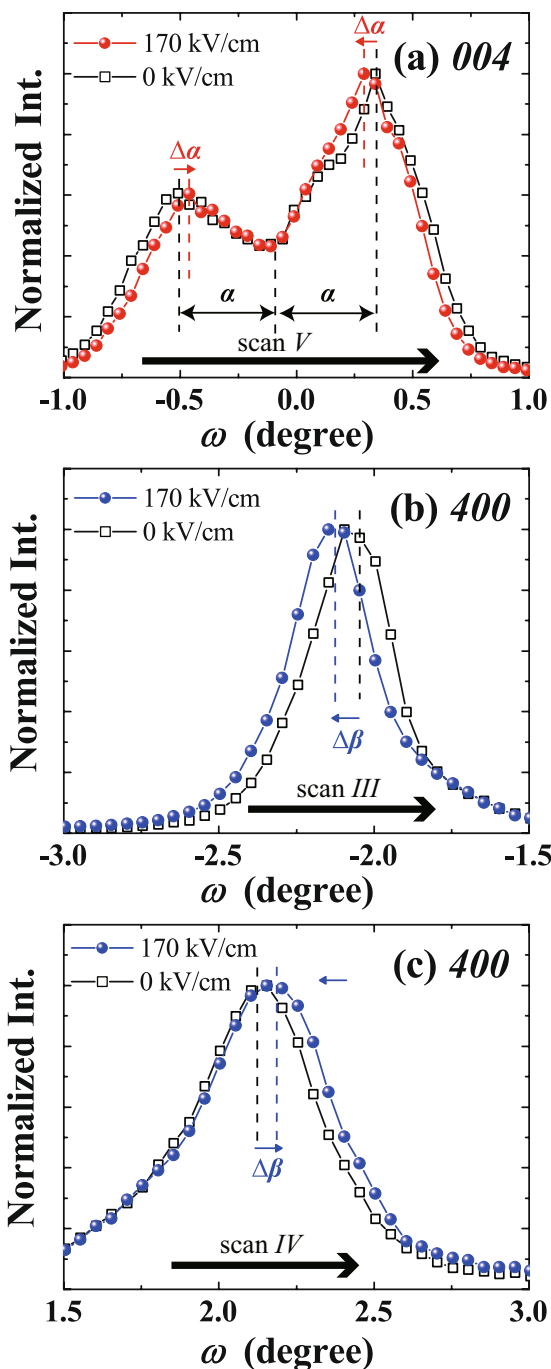


**Figure 3.** Rocking curves ( $\omega$  scans) of (a) 004 PZT under 0 kV/cm (open squares) and 170 kV/cm (filled circles) in scan V in Fig. 1(b). (b,c) Rocking curve of 400 PZT under 0 kV/cm (open squares) and 170 kV/cm (filled circles) of image in (b) scan III and (c) scan IV in Fig. 1(a), respectively.

derivative for the charge, which is the current flowing through the electric circuit, is shown in Fig. 4(e). Two peaks correspond to the current associated with applying and removing an electric field. The transition duration, which is defined as the time over which a current with an absolute value larger than the noise level of 0.002 mA flows, is approximately 40 ns for both application and removal. This duration time includes both rise time, determined by the limitation of the current pulse generator, and transient time, determined by impedance of the electric circuit. Conversely, Fig. 4(b)-(d) show that the elastic deformation, tilting motion, and ferroelastic domain switching seem to have been completed within 40 ns because each spectrum has only one single data point during the change in electric field that corresponds to these transition states. As previous studies reported<sup>13</sup>, the tilting angle is closely related to the volume fractions of each domain and tetragonality of the crystal lattice. This change in tilting angle indicates the change in the volume fraction of *c*-domain. Unfortunately, the volume fraction of domains cannot be estimated by the time dependent intensities of 400 and 004 peaks due to complexity of the

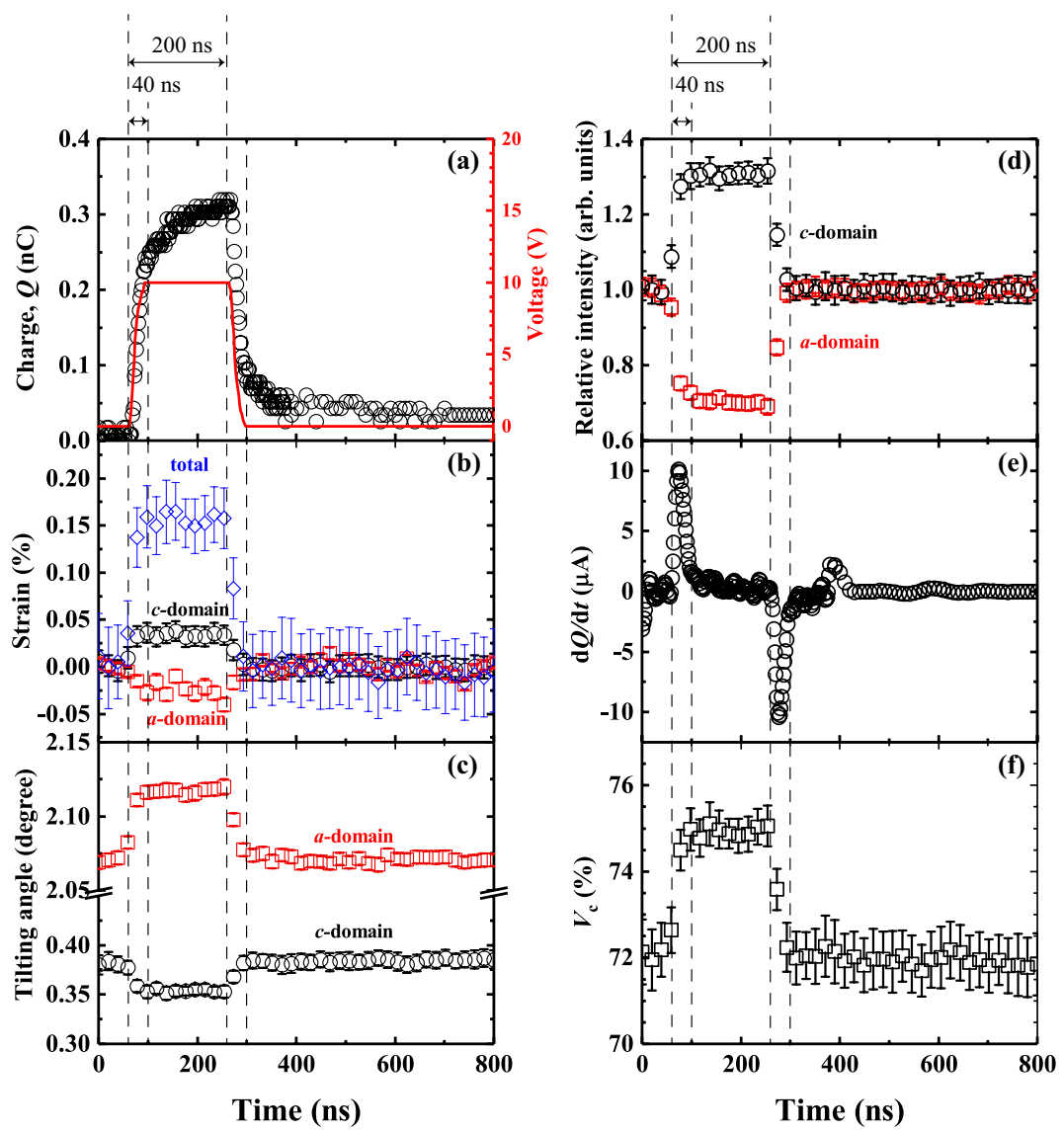


**Figure 4.** (a) Capacitance and (e) calculated differential capacitance by time as a function of time during application of a 200-ns pulsed electric field with a magnitude of 170 kV/cm. The solid line in panel (a) indicates applied pulse voltage measured by reference capacitor. (b) Strain, (c) tilting angle, (d) intensity, and (f)  $V_c$  of PZT 400 (circles) and PZT 004 (squares) peaks as a function of time during application of a 200-ns pulsed electric field with a magnitude of 170 kV/cm. Intensities are integrated one obtained by peak fitting. Open circles and squares are calculated by the 004 diffraction peak from the *c*-domain and the 400 diffraction peak from the *a*-domain, respectively. Total strain including extrinsic contribution (open diamond) was also plotted in panel (b).

domain structures. But the increase and decrease in integrated intensities of 004 and 400 peaks, respectively, strongly support the domain switching from *a*-domain to *c*-domain. When the field was removed, tilt angles and intensities return back to their original positions at zero field at less than 40 ns as well. These data were acquired during the repetitive application of electric pulses of 800-ns duration confirming that the observed changes in tilt angles and intensities and hence a ferroelastic domain wall motions is perfectly repeatable. More importantly all these motions (charge, lattice strain, domain switching, and change in tilting angle) occur simultaneously without delay when the electric field across the PZT film changed. This means that the 90° domain switching from (100) to (001) can be exploited to enhance the piezoresponse response even on the order of several tens of nanoseconds. It should be noted that the response time in this study is less than that of previously reported data, which is on the order of hundreds of nanoseconds<sup>16, 17</sup>. Moreover, the non-180° ferroelastic domain motion for thin films does not suffer from frequency dispersion as seen in bulk ceramics<sup>18</sup>, where it becomes inactive for short such ns pulse time. One possible explanation could be that the electric fields applied to the film are one order higher than those applied to the ceramics, which may have enabled us to achieve high-speed non-180° domain switching. Additionally non-180° domain switching by an electric field can be also influenced by strains of the grain that are accumulated in polycrystalline ceramic bodies. These are changed by grain size, grain shape, and grain-to-grain disorientation in neighbour grains<sup>26</sup>.

Finally, it is worth noting to compare the strain evaluated from the present *in-situ* XRD and strain-electric-field measurement (see Fig. S3) by applying unipolar electric field with 5 Hz. The figure shows that the almost linear response of strain with respect to electric field, indicating piezoelectric coefficient ( $d_{33\text{obs}}$ ) of around 100 pC/N. The volume fraction change in *c*-domain calculated from tilting angle and total strain as a function of time during *in-situ* XRD measurements are plotted in Fig. 4(f) and (b), respectively. The piezoelectric coefficient ( $d_{33\text{XRD}}$ ) obtained from the XRD measurement is around 86 pC/N, showing reasonable agreement with the value obtained by strain - electric field measurements. This consistency between them again confirms that the ferroelastic domain switching here does not suffer from strong frequency dispersion previously observed for 90° domain switching<sup>18</sup>.

Note that the intrinsic component, which indicates the lattice deformation of *c*-domain by electric field, is only 17 pC/N, of which contribution for total  $d_{33\text{XRD}}$  is around 20%. That is domain switching from *a*-domain to *c*-domain dominates the total piezoelectric response. Our observation of fast 90° domain switching opens up exciting new possibilities for ultrafast electromechanical switches and sensors that including piezoelectric transistor applications that rely on 90° domain wall motion<sup>27</sup>.

## Conclusion

In summary, we used time-resolved synchrotron XRD in conjunction with a high-speed pulse generator to demonstrate the average lattice and domain motions as well as the tilting angle of the domains. The 90° domain can be switched by a 200-ns-wide electric field. The change in tilt angles of  $\Delta\alpha = 0.05^\circ$  in the *a*-domain and  $\Delta\beta = -0.03^\circ$  in the *c*-domains were observed under an applied electric field, commensurate with a change in  $V_c$  and tetragonality ( $c/a$ ). Moreover, reversible 90° occurs within 40 ns, a limit set by our present electrical set up. This opens up exciting new possibilities for ultrafast electromechanical switches and sensors that rely on 90° domain wall motion.

## Methods

$\text{Pb}(\text{Zr}_{0.4}\text{Ti}_{0.6})\text{O}_3$  [PZT] films, 600 nm in thickness, grown on (100)<sub>c</sub>SrRuO<sub>3</sub>-coated (100) KTaO<sub>3</sub> substrates by pulsed-metal organic chemical vapour deposition (MOCVD) were used for measurements. Details of the sample preparation are given elsewhere<sup>28</sup>. SrRuO<sub>3</sub>, which was indexed by a pseudo-cubic notation like  $hkl_{pc}$  here, was grown by a RF-magnetron sputtering method reported in our previous paper<sup>29</sup>. For applying an electric field to this film, Pt top electrodes 100  $\mu\text{m}$  in diameter were fabricated on the PZT films by electron-beam evaporation.

To determine the structural characterisations of the PZT films before applying an electric field, high-resolution X-ray diffraction (HRXRD) and  $2\theta - \omega$  mapping were performed with a 12.4-keV X-ray beam at the National Institute for Materials Science (NIMS) beam line, BL15XU, of SPring-8, Japan.

*In-situ* observation of the change in lattice parameters and domain structure with an applied electric field was carried out at the BL13XU at SPring-8 for Pt/PZT/SrRuO<sub>3</sub> capacitors. To acquire the electric field-induced changes in diffraction data, an incident beam with photon energy of 12.4 keV was focused down to a few micrometres in width and height using a two-dimensional focusing refractive lens and irradiated on the Pt top electrode with the help of a fluorescent X-ray detector. We applied pulse voltages with a magnitude of 10 V and monitored the changes in 400 and 004 diffraction peaks. A positive 10-V square pulsed voltage 200 ns in width was applied to the capacitor to obtain sufficient poling treatment prior to measurement. The 200-ns square pulsed electric field was applied using a pulse generator (Agilent, 8114 A) and FCE-HS3 (Toyo, 6321). Time-resolved X-ray diffraction was measured using a high-speed avalanche photodiode detector (APD). The pulse height generated by a time-to-amplitude converter (ORTEC 567), for which X-ray pulse measured by the APD detector was used as a start signal and pulse signal synchronized to the electric pulse applied to the PZT films was used as a stop signal, is canalized by a multi-channel analyser. This technique cannot detect more than one photon for one period, so that properly attenuated X-rays were irradiated. No remarkable fatigue was confirmed during measurements (see Fig. S4). Detailed description of the time-resolved synchrotron X-ray diffraction measurement is given elsewhere<sup>30</sup>.

## References

- Muralt, P. Ferroelectric thin films for micro-sensors and actuators: a review. *J. Micromech. Microeng.* **10**, 136 (2000).
- Jones, J. L., Slavovitch, E. B. & Bowman, K. J. Domain texture distributions in tetragonal lead zirconate titanate by x-ray and neutron diffraction. *J. Appl. Phys.* **97**, 034113 (2005).
- Kim, D.-J., Maria, J.-P., Kingon, A. I. & Streiffer, S. K. Evaluation of intrinsic and extrinsic contributions to the piezoelectric properties of  $\text{Pb}(\text{Zr}_{1-x}\text{T}_x)\text{O}_3$  thin films as a function of composition. *J. Appl. Phys.* **93**, 5568 (2003).
- Nagarajan, V. *et al.* Dynamics of ferroelastic domains in ferroelectric thin films. *Nat Mater* **2**, 43–47 (2003).
- Lee, K. S., Kim, Y. K., Baik, S., Kim, J. & Jung, I. I. S. *In situ* observation of ferroelectric 90°-domain switching in epitaxial  $\text{Pb}(\text{Zr}, \text{Ti})\text{O}_3$  thin films by synchrotron x-ray diffraction. *Appl. Phys. Lett.* **79**, 2444 (2001).
- Gao, P. *et al.* Ferroelastic domain switching dynamics under electrical and mechanical excitations. *Nat. Commun.* **5**, 3801 (2014).
- Ganpule, C. S. *et al.* Role of 90° domains in lead zirconate titanate thin films. *Appl. Phys. Lett.* **77**, 292 (2000).
- Li, W. & Alexe, M. Investigation on switching kinetics in epitaxial  $\text{Pb}(\text{Zr}_{0.2}\text{Ti}_{0.8})\text{O}_3$  ferroelectric thin films: Role of the 90° domain walls. *Appl. Phys. Lett.* **91**, 262903 (2007).
- Lee, J. K. *et al.* Direct observation of asymmetric domain wall motion in a ferroelectric capacitor. *Acta Mater.* **61**, 6765–6777 (2013).
- Roytburd, A. L., Alpay, S. P., Bendersky, L. A., Nagarajan, V. & Ramesh, R. Three-domain architecture of stress-free epitaxial ferroelectric films. *J. Appl. Phys.* **89**, 553 (2001).
- Kwak, B. S. *et al.* Domain formation and strain relaxation in epitaxial ferroelectric heterostructures. *Phys. Rev. B* **49**, 14865–14879 (1994).
- Speck, J. S., Daykin, A. C., Seifert, A., Romanov, A. E. & Pompe, W. Domain configurations due to multiple misfit relaxation mechanisms in epitaxial ferroelectric thin films. III. Interfacial defects and domain misorientations. *J. Appl. Phys.* **78**, 1696 (1995).
- Nakaki, H. *et al.* Strain-relaxed structure in (001)/(100)-oriented epitaxial  $\text{Pb}(\text{Zr}, \text{Ti})\text{O}_3$  films grown on (100) SrTiO<sub>3</sub> substrates by metal organic chemical vapor deposition. *J. Appl. Phys.* **105**, 014107 (2009).

14. Grigoriev, A. *et al.* Nanosecond domain wall dynamics in ferroelectric Pb(Zr, Ti)O<sub>3</sub> thin films. *Phys. Rev. Lett.* **96**, 187601 (2006).
15. Grigoriev, A. *et al.* Subnanosecond piezoelectric x-ray switch. *Appl. Phys. Lett.* **89**, 021109 (2006).
16. Ehara, Y. *et al.* Ultrafast switching of ferroelastic nanodomains in bilayered ferroelectric thin films. *Appl. Phys. Lett.* **99**, 182906 (2011).
17. Huang, H.-H. *et al.* Epitaxial PbZr<sub>x</sub>Ti<sub>1-x</sub>O<sub>3</sub> Ferroelectric Bilayers with Giant Electromechanical Properties. *Adv. Mater. Interfaces* **2**, 1500075 (2015).
18. Seshadri, S. B., Prewitt, A. D., Studer, A. J., Damjanovic, D. & Jones, J. L. An *in situ* diffraction study of domain wall motion contributions to the frequency dispersion of the piezoelectric coefficient in lead zirconate titanate. *Appl. Phys. Lett.* **102**, 042911 (2013).
19. Stemmer, S. *et al.* The influence of Pt and SrTiO<sub>3</sub> interlayers on the microstructure of PbTiO<sub>3</sub> thin films deposited by laser ablation on (001) MgO. *J. Mater. Res.* **10**, 791–794 (1995).
20. Foster, C. M. *et al.* Substrate effects on the structure of epitaxial PbTiO<sub>3</sub> thin films prepared on MgO, LaAlO<sub>3</sub>, and SrTiO<sub>3</sub> by metalorganic chemical-vapor deposition. *J. Appl. Phys.* **78**, 2607–2622 (1995).
21. Yasui, S. *et al.* Complex domain structure in relaxed PbTiO<sub>3</sub> thick films grown on (100)cSrRuO<sub>3</sub>//(100)SrTiO<sub>3</sub> substrates. *J. Appl. Phys.* **112**, 052001 (2012).
22. Utsugi, S. *et al.* Domain structure of (100)/(001)-oriented epitaxial PbTiO<sub>3</sub> thick films with various volume fraction of (001) orientation grown by metal organic chemical vapor deposition. *Appl. Phys. Lett.* **94**, 052906 (2009).
23. Nakaki, H. *et al.* Experimental evidence of strain relaxed domain structure in (100)/(001)-oriented epitaxial lead titanate thick films grown by metal organic chemical vapor deposition. *J. Appl. Phys.* **104**, 064121 (2008).
24. Kim, Y. K. *et al.* Domain structures and piezoelectric properties in epitaxial Pb(Zr<sub>0.35</sub>Ti<sub>0.65</sub>)O<sub>3</sub> thin films. *Appl. Phys. Lett.* **88**, 252904 (2006).
25. Ganpule, C. S. *et al.* Imaging three-dimensional polarization in epitaxial polydomain ferroelectric thin films. *J. Appl. Phys.* **91**, 1477 (2002).
26. Pramanick, A., Damjanovic, D., Daniels, J. E., Nino, J. C. & Jones, J. L. Origins of Electro-Mechanical Coupling in Polycrystalline Ferroelectrics During Subcoercive Electrical Loading. *J. Am. Ceram. Soc.* **94**, 293–309 (2011).
27. Newns, D. M., Elmegreen, B. G., Liu, X.-H. & Martyna, G. J. The piezoelectronic transistor: A nanoactuator-based post-CMOS digital switch with high speed and low power. *MRS Bull.* **37**, 1071–1076 (2012).
28. Nagashima, K., Aratani, M. & Funakubo, H. Improvement of Property of Pb(Zr<sub>x</sub>Ti<sub>1-x</sub>)O<sub>3</sub> Thin Film Prepared by Source Gas Pulse-Introduced Metalorganic Chemical Vapor Deposition. *Jpn. J. Appl. Phys.* **39**, L996–L998 (2000).
29. Kamo, T. *et al.* RF Magnetron Sputtering Growth of Epitaxial SrRuO<sub>3</sub> Films with High Conductivity. *Jpn. J. Appl. Phys.* **46**, 6987–6990 (2007).
30. Sakata, O. *et al.* *In-situ* lattice-strain analysis of a ferroelectric thin film under an applied pulse electric field. *AIP Conf. Proc.* **1234**, 151–154 (2010).

## Acknowledgements

This study was partially supported by KAKENHI (15H04121(JSPS) and 26220907 (JSPS)) and PRESTO(JPMJPR16R9), JST. The XRD measurements were performed by the NIMS beamline BL15XU at SPring-8 under Proposals No. 2012B4904 and 2014B4909 as part of the NIMS Nanotechnology Platform (Projects No. A-12-NM-0033 and A-14-NM-0119) on microstructural characterization, respectively. They were also performed at the BL13XU with the approval of the Japan Synchrotron Radiation Research Institute (Proposal Nos. 2012B1034, 2012B1656, and 2013A4713) RM and NV thank the ARC Linkage and ARC Discovery program.

## Author Contributions

Y.E. synthesised the sample. Y.E. and H.F. wrote the main manuscript. S.Y., T.O., T. Shimizu, T. Shiraishi, H.T., N.K., R.M., and T.Y. performed the measurements. Y.E. and T. Shimizu performed the analysis. S.Y. and O.S. designed the experiments, Y.I. and O.S. supervised the *in-situ* measurements, and N.V. and H.F. supervised the research. All authors discussed the results and contributed to the manuscript.

## Additional Information

**Supplementary information** accompanies this paper at doi:[10.1038/s41598-017-09389-6](https://doi.org/10.1038/s41598-017-09389-6)

**Competing Interests:** The authors declare that they have no competing interests.

**Publisher's note:** Springer Nature remains neutral with regard to jurisdictional claims in published maps and institutional affiliations.



**Open Access** This article is licensed under a Creative Commons Attribution 4.0 International License, which permits use, sharing, adaptation, distribution and reproduction in any medium or format, as long as you give appropriate credit to the original author(s) and the source, provide a link to the Creative Commons license, and indicate if changes were made. The images or other third party material in this article are included in the article's Creative Commons license, unless indicated otherwise in a credit line to the material. If material is not included in the article's Creative Commons license and your intended use is not permitted by statutory regulation or exceeds the permitted use, you will need to obtain permission directly from the copyright holder. To view a copy of this license, visit <http://creativecommons.org/licenses/by/4.0/>.

© The Author(s) 2017